Journal of Power Sources 192 (2009) 144–150

Contents lists available at ScienceDirect

Journal of Power Sources

journal homepage: www.elsevier.com/locate/jpowsour

Effect of the support properties on the preparation and performance of platinum catalysts supported on carbon nanofibers

L. Calvillo[a], M. Gangeri[b], S. Perathoner[b], G. Centi[b], R. Moliner[a], M.J. Lázaro[a,*]

[a] Instituto de Carboquímica (CSIC), Miguel Luesma Castán 4, 50018 Zaragoza, Spain
[b] Dipartimento di Chimica Industriale ed Ingegneria dei Materiali, Università di Messina, Salita Sperone 31, 98166 Messina, Italy

ARTICLE INFO

Article history:
Received 23 December 2008
Accepted 8 January 2009
Available online 19 January 2009

Keywords:
Carbon nanofibers
Morphology
Surface chemistry
Electrocatalyst
PEMFC

ABSTRACT

Platinum nanoparticles were supported on carbon nanofibers (CNFs) for their use as electrocatalyst for PEM fuel cells. Before platinum deposition, CNFs were oxidized using concentrated HNO_3 or a HNO_3–H_2SO_4 mixture as oxidizing agents. During these treatments, new surface oxygen groups were created. Moreover, the most severe treatments resulted in the shortening of CNFs. Both effects allow to study the influence of both the morphology and the surface chemistry of CNFs on the preparation and performance of Pt electrocatalysts. Catalysts were prepared by the incipient wetness impregnation method. CNFs and electrocatalysts were characterized by X-ray diffraction (XRD), transmission electron microscopy (TEM) and N_2-physisorption. Furthermore, the performance of Pt/CNF based electrodes was compared with that of a commercial Pt/carbon black electrode (E-TEK) in a 1-cm^2 PEM fuel cell.

The results showed that both the surface chemistry and the morphology of the support have an important effect on the dispersion, particle size and activity of Pt catalysts. An increase in the agglomeration degree of Pt particles as the severity of oxidation treatments increased was observed. However, the performance of Pt/CNF electrodes was better than that of the commercial one. This was attributed to the CNF porous structure and to the better Pt–support interaction through the surface oxygen groups of the support.

1. Introduction

Among the different types of fuel cells, polymer electrolyte fuel cells, PEFCs (PEMFCs and DMFCs) are the most promising for both portable and stationary applications due to its advantageous features such as high power density at low temperatures (55–95 °C), low weight, compactness, and suitability for discontinuous operation [1,2]. However, the cost must be reduced and several technological challenges must be solved before PEFCs can start to be used extensively. The fuel cell catalyst is the major contributor to these difficulties. Therefore, the major task in moving toward fuel cell commercialization is the development of breakthrough catalysts, improvement of catalyst activity, stability and durability, and the reduction of catalyst cost [2–4].

At present, the most effective fuel cell catalysts are highly dispersed platinum-based nanoparticles. These Pt nanoparticles are normally supported on carbon materials in order to increase the active surface area of Pt and improve the catalyst utilization.

Nowadays, among all kinds of carbon supports, carbon blacks are the most commonly used due to their high mesoporous distribution and their graphite characteristics. Vulcan XC-72 is the most frequently used because of its good compromise between electrical conductivity and high specific surface area [5,6]. Recently, however, novel non-conventional carbon materials such as carbon nanofibers and nanotubes [7,8], carbon xerogels and aerogels [9,10], and ordered mesoporous carbons [11,12], have been proposed as platinum supports that can achieve uniform and highly dispersed Pt loadings.

Among these carbon materials, carbon nanofibers (CNFs) have attracted a great attention as electrocatalyst support due to their unique textural, mechanical and electrical properties. Due to their morphology, CNFs have been used as electrocatalyst support without any pre-treatment. This is due to the edges of graphite planes can serve as suitable sites for the stabilization of small platinum particles [13]. CNFs have been used as Pt and PtRu support. These carbon nanofibers-based catalysts showed a better performance than the conventional catalysts supported on Vulcan XC-72 [7,14,15]. However, the last studies about the use of CNFs as electrocatalyst support are aimed at optimizing their surface chemistry in order to improve the metal–support interaction. Due to their inert nature, CNFs contain only a small number of surface oxygen groups. However, their surface chemistry can be modified by oxidation treatments in a gas or liquid phase in order to create functional groups [16–18]. These functional groups can significantly affect

* Corresponding author. Tel.: +34 976 733977; fax: +34 973 733318.
E-mail address: mlazaro@icb.csic.es (M.J. Lázaro).

0378-7753/$ – see front matter © 2009 Elsevier B.V. All rights reserved.
doi:10.1016/j.jpowsour.2009.01.005

the manufacture and performance of electrocatalysts, and they are responsible for both the acid–base and the redox properties of the CNFs. However, the effect of these groups on the dispersion and anchoring of the platinum is not well established. Some authors have determined that the presence of surface oxygen groups is necessary to achieve a good Pt dispersion [19,20], whereas others argue that they do not influence, or have a negative effect, on the dispersion of the active phase [21].

In addition, research has also shown that the surface chemistry of the support influences the performance of the electrocatalysts. Carbon supports are not inert materials. During the electrochemical reactions, the metal–support interaction is attributed to the presence of a platinum–support electronic effect. The specific metal–support interaction involves electron transfer from platinum clusters to oxygen atoms on the support surface [2]. This interaction is considered to be beneficial to the enhancement of the catalytic properties and to improve electrocatalyst's stability. However, the functionalization of the support results in a decrease of its electrical conductivity. Therefore, since the functionalization process seems to have opposite effects on the performance of the catalysts, further study is needed.

In this work, carbon nanofibers are proposed as support for preparing platinum electrocatalysts. From a previous study about the functionalization of carbon nanofibers [16], CNFs with different morphology and surface chemistry have been selected and used as electrocatalyst support. This allows to study the influence of both their morphology and their surface chemistry on the preparation and performance of Pt electrocatalysts. Supports and electrocatalysts have been characterized by transmission electron microscopy (TEM), N_2-physisorption and X-ray diffraction (XRD). Furthermore, the performance of Pt/CNF catalysts based electrodes has been compared with that of a commercial Pt/carbon black electrode (E-TEK) in a 1-cm^2 PEM fuel cell.

2. Experimental

2.1. Synthesis and functionalization of carbon nanofibers

CNFs were synthesized via the thermocatalytic decomposition (TCD) of methane over a Ni:Cu:Al_2O_3 catalyst [22]. Prior to synthesis, catalyst was reduced in a pure H_2 flow for 3 h at 550 °C. CNFs were then grown in a pure methane flow at 700 °C for 10 h. Subsequently, the surface chemistry of synthesized CNFs was modified by means of different oxidation treatments in liquid phase, using concentrated HNO_3 (CNF Nc) and a HNO_3:H_2SO_4 1:1 (v/v) mixture (CNF NS) as oxidizing agents. The oxidation treatments were carried out at room (T_a) and boiling temperature (T_b) for 0.5 and 2 h [16].

2.2. Preparation of the electrocatalysts

Platinum catalysts were prepared by the incipient wetness impregnation method using H_2PtCl_6 as metal precursor. Theoretical platinum content in the catalysts was fixed in 20 wt%. Subsequently, platinum was reduced in a pure H_2 flow at 300 °C for 2 h.

2.3. Preparation of membrane and electrodes assembly (MEA)

Several MEAs were prepared for electrochemical measurements using different electrodes as anode and a commercial electrode (E-TEK Inc.) as cathode (Pt, 0.4–0.6 mg cm^{-2}). The commercial electrode of E-TEK was based on Pt deposited on Vulcan XC-72, which was then deposited on the carbon cloth gas diffusion membrane (GDM). The anode electrodes were prepared by depositing a suspension of Nafion solution and the synthesized electrocatalyst (Nafion content = 32 wt%) on pieces of E-TEK ELAT carbon cloth (the same than that used in the commercial electrode). The final amount of metal active phase in all the prepared electrodes was approximately 0.5 mg cm^{-2}, for their comparison with the commercial electrode E-TEK.

Before the MEAs preparation, the polymer electrolyte membrane, Nafion® 115 (Du Pont Chemical), was cleaned by immersing in 3% H_2O_2 for 1 h at 80 °C to remove organic impurities and subsequently, in a 0.5-M H_2SO_4 solution for 1 h at 80 °C. H_2SO_4 was removed by washing in boiling distilled water.

The final assembly of the electrodes and the Nafion membrane was hot pressed between two metallic plates and heated at 120 °C, with a pressure of 20 kg cm^{-2} for 90 s.

2.4. Characterization methods

XRD patterns for the determination of Pt morphology and crystallite size were recorded using a Bruker AXS B8 Advance diffractometer with θ–θ configuration and using Cu K_α radiation.

TEM images for the determination of the distribution and size of platinum particles were obtained using a 300-kV Philips CM-30 TEM. Images were recorded with a Multi Scan CCD camera (model 794, Gatan) using lose-dose conditions.

Nitrogen adsorption–desorption isotherms were measured at −196 °C using a Micromeritics ASAP 2020. Total surface area and pore volume were determined using the BET equation and the single point method, respectively. Pore size distribution curves were calculated by BJH method, and the position of the maximum was used as the average pore diameter.

Platinum loading was determined by ICP-OES. Electrocatalysts were calcined at 600 °C for 4 h and then dissolved in 10 cm^3 HNO_3 (65%) and 30 cm^3 HCl (37%). The obtained solution was transferred into a 100-cm^3 calibrated flask and the volume completed with deionised water. Then the solutions were analyzed using ICP-OES Jobin Yvon 2000.

2.5. Electrochemical studies

Electrocatalytic activity measurements were carried out in a PEM fuel cell (geometric area 1 cm^2) working at room temperature and atmospheric pressure. Hydrogen and oxygen were passed through humidifiers to wet the gases, in order to maintain the high ionic conductivity of the Nafion membrane, and fed at the anode and the cathode at a flow rate of 9 and 50 ml min^{-1}, respectively. Characteristic polarization curves V (cell potential) versus I (current density) for each of the prepared MEAs were measured under strictly comparable conditions. MEA prepared with the E-TEK electrode (Pt, 0.4–0.6 mg cm^{-2}) using the same method was tested for comparison. The polarization curves were recorded connecting the two electrodes electrochemical cell to a potentiostat/galvanostat (AMEL 2049), where the anode represented both reference and counter electrode and the cathode acted as working electrode. The electrochemical measurements were carried out in galvanostatic way, setting negative polarity of the working electrode with respect to the reference one and taking the cell potential by varying the electric load.

3. Results and discussion

3.1. Effect of the oxidation treatments on the carbon nanofibers properties

In a previous work, herringbone carbon nanofibers were treated with HNO_3 or HNO_3:H_2SO_4 (1:1, v/v) in order to modify their surface chemistry, creating surface oxygen groups [16].

The surface chemistry of CNFs was studied by temperature programmed desorption (TPD) experiments. These experiments give

Table 1
Quantification of surface oxygen groups as CO and CO_2 amounts desorbed during the TPD experiments.

Sample	CO_2 (μmol g^{-1})	CO (μmol g^{-1})	CO_2 + CO (μmol g^{-1})	CO/CO_2
CNF	31	221	252	6.9
CNF NSTa0.5	167	376	543	2.2
CNF NcTb0.5	314	619	933	1.9
CNF NSTb0.5	575	715	1290	1.2
CNF NcTb2	489	744	1233	1.5
CNF NSTb2	1956	1398	3354	0.7

information about the surface oxygen groups created during the oxidation treatments. Acidic groups (carboxylic groups, lactones and anhydrides) are decomposed into CO_2 at lower temperatures and basic and neutral groups (anhydrides, phenols and quinones) are decomposed into CO at higher temperatures [23]. TPD results showed that an increase in the severity of oxidation treatments resulted in an increase in the number of surface oxygen groups (Table 1). Treatment with HNO_3–H_2SO_4 at boiling temperature was the most effective at creating functional groups.

It is expected that these surface oxygen groups have two functions during the catalyst preparation by the incipient wetness impregnation method. On one hand, it is expected that they decrease the hydrophobic character of CNFs, improving their interaction with the metal precursor during the impregnation stage. And on the other hand, it is expected that they act as metal anchoring sites, hindering the redistribution and agglomeration of platinum particles during the metal precursor reduction stage.

The oxidation treatments also modified the morphology of CNFs (observed by SEM but not shown). The most severe treatments resulted in the shortening of CNFs (CNF NcTb2, CNF NSTb0.5 and CNF NSTb2). This effect was more noticeable as increasing the severity of the oxidation treatments. However, neither their textural properties nor the average pore diameter (around 7 nm) were significantly affected, as seen in Table 2.

From this functionalization study, some samples with different properties were selected for the preparation of Pt electrocatalysts in order to study the effect of both the morphology and the surface chemistry of CNFs. Selected samples are described in Table 3. The first group was made up of nanofibers that maintained their original morphology after the oxidation treatments and presented different functionalization grades (CNF, CNF NSTa0.5 and CNF NcTb0.5). The second group was made up of nanofibers with similar surface chemistry and different morphology (from the SEM observations) (CNF NcTb0.5, CNF NcTb2 and CNF NSTb0.5). Finally, CNF NSTb2 sample was selected due to its special characteristics, namely, the large number of surface oxygen groups and partially destroyed morphology.

Table 3
Selected carbon nanofibers used as electrocatalyst support.

Sample	Oxidizing agent	Temperature (°C)	Time (h)
CNF	–	–	–
CNF NSTa0.5	HNO_3–H_2SO_4 1:1 (v/v)	25	0.5
CNF NcTb0.5	Concentrated HNO_3 (65%)	115	0.5
CNF NcTb2	Concentrated HNO_3 (65%)	115	2
CNF NSTb0.5	HNO_3–H_2SO_4 1:1 (v/v)	115	0.5
CNF NSTb2	HNO_3–H_2SO_4 1:1 (v/v)	115	2

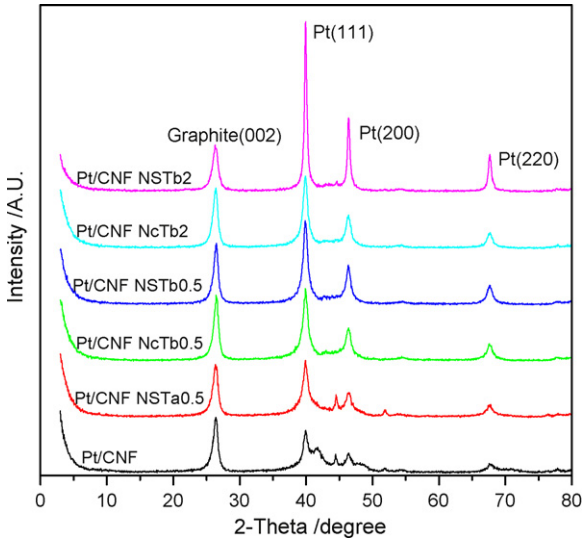

Fig. 1. XRD patterns of platinum catalysts supported on CNFs with different functionalization grade.

3.2. Physicochemical characterization of the electrocatalysts

The morphological and crystallographic properties of the prepared electrocatalysts were studied by XRD. XRD patterns of Pt nanoparticles supported on CNFs are reported in Fig. 1. All samples showed the characteristic diffraction peaks of the fcc structure of the platinum. This indicates the successful reduction of the Pt precursor to metallic form. In addition, a diffraction peak at 26.2° was observed, which is associated to the graphitic structure of the carbon nanofibers used as support.

The average Pt crystallite size was estimated from the Pt reflections by the Scherrer's equation (Table 4) following the method described in [24]. Pt particles supported on unoxidized carbon nanofibers had an average size of about 3 nm. This value is in good agreement with those reported in the literature for the preparation of platinum catalysts supported on carbon nanofibers [15,19,20],

Table 2
Textural parameters of carbon nanofibers and Pt/CNF electrocatalysts.

Sample	S_{BET} (m^2 g^{-1})	V_{total} (cm^3 g^{-1})	$V_{micropore}$ (cm^3 g^{-1})	$V_{mesopore}$[a] (cm^3 g^{-1})	$S_{micropore}$ (m^2 g^{-1})	$S_{mesopore}$[a] (m^2 g^{-1})
CNF	95.7	0.23	0.001	0.23	4.0	91.7
CNF NSTa0.5	102.7	0.22	0.003	0.21	7.6	95.1
CNF NcTb0.5	102.5	0.21	0.004	0.21	7.8	94.7
CNF NSTb0.5	105.4	0.23	0.004	0.23	8.2	97.2
CNF NcTb2	119.9	0.28	0.004	0.28	8.4	111.5
CNF NSTb2	96.3	0.22	0.003	0.22	5.8	90.5
Pt/CNF	80.5	0.17	0.004	0.16	7.2	73.3
Pt/CNF NSTa0.5	86.3	0.22	0.003	0.21	6.6	79.7
Pt/CNF NcTb0.5	81.1	0.23	0.005	0.23	9.4	71.7
Pt/CNF NSTb0.5	84.2	0.24	0.006	0.23	10.7	73.5
Pt/CNF NcTb2	81.1	0.25	0.004	0.24	8.1	73.0
Pt/CNF NSTb2	109.6	0.23	0.003	0.23	6.4	103.2

[a] Calculated from the difference between the total and micropore values.

Table 4
Average platinum crystallite size calculated from the XRD pattern using the Scherrer's equation.

Sample	Pt size (nm)
Pt/CNF	3.0
Pt/CNF NSTa0.5	6.1
Pt/CNF NcTb0.5	8.2
Pt/CNF NSTb0.5	9.6
Pt/CNF NcTb2	9.9
Pt/CNF NSTb2	23

which stated that the stabilization of small platinum crystals is associated to the carbon nanofibers structure [13].

As observed in Fig. 1, a decrease in the Pt reflections width was observed as the severity of the oxidation treatments of the CNFs increased. This indicated that Pt crystallites became larger as the number of oxygen surface groups of the support increased. However, the crystallite size was small (6–9 nm), except for the catalyst supported on the most severe treated CNFs (Pt/CNF NSTb2) that had Pt crystallites of about 23 nm. This is attributed to both the partially destroyed morphology and the high number of surface oxygen groups of carbon nanofibers.

From these results, the effect of both the morphology and surface chemistry of CNFs on the Pt crystallite size can be studied. The effect of the morphology of the carbon nanofibers can be analyzed taking Pt/CNF NcTb0.5, Pt/CNF NSTb0.5 and Pt/CNF NcTb2 samples into account, since the textural properties and the surface chemistry of the supports were very similar. As can be seen in Table 4, the Pt crystallite size increased from 8.2 to 9.9 nm according to Pt/CNF NcTb0.5 < Pt/CNF NSTb0.5 < Pt/CNF NcTb2. This increase is related to the shortening grade of CNFs during the oxidation treatments (CNF NcTb0.5 < CNF NSTb0.5 < CNF NcTb2). Therefore, it can be determined that the CNFs morphology is important to obtain small metal crystallites.

On the other hand, the effect of the surface chemistry of the support on the Pt crystallite size can be established taking Pt/CNF, Pt/CNF NSTa0.5 and Pt/CNF NcTb0.5 samples into account, since the supports maintained the original CNFs morphology. An increase in the platinum crystallite size from 3 to 8.2 nm was observed as the number of surface oxygen groups increased. This increase was proportional to the number of functional groups.

From these results, it can be deduced that both the morphology and the surface chemistry of the support influence the Pt crystallite size. This was confirmed by the results obtained for the Pt/CNF NSTb2 catalyst. Pt crystallites had an average size of about 23 nm, which is attributed to the effect of both properties, that is, the high number of surface oxygen groups and the partially destroyed morphology of the support.

The size and distribution of platinum particles were also studied by TEM. Figs. 2–4 show the TEM images obtained for different Pt/CNF based catalysts. In Fig. 2a, it is observed that a uniform distribution of Pt particles was achieved by the incipient wetness impregnation method. Pt particles supported on the unoxidized carbon nanofibers were approximately 3 nm in diameter, which is in concert with XRD results. In addition, Pt particles showed a highly crystalline faceted structure (Fig. 2b) that can be associated with a strong metal-support interaction [25,26]. For catalyst supported on oxidized CNFs, the formation of some Pt agglomerates

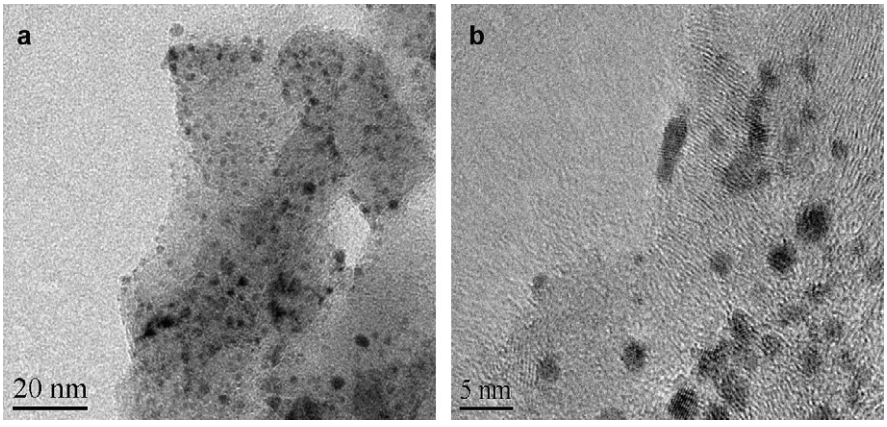

Fig. 2. TEM images of platinum catalyst supported on the unoxidized CNFs (Pt/CNF).

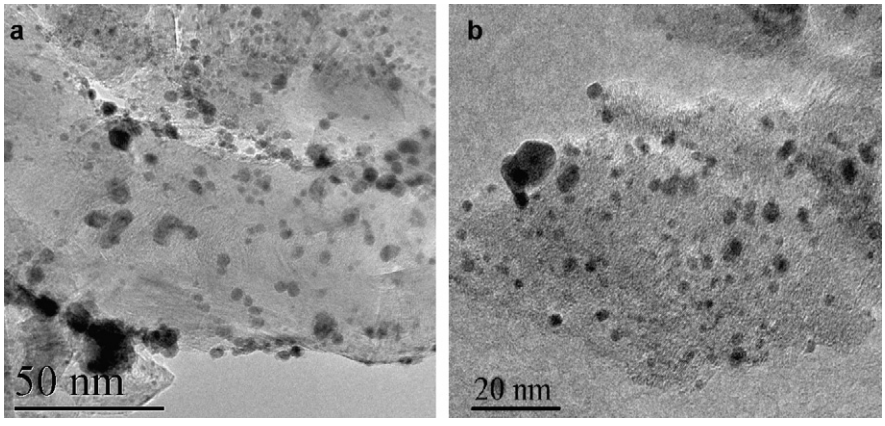

Fig. 3. TEM images of platinum catalyst supported on oxidized CNFs (Pt/CNF NSTa0.5).

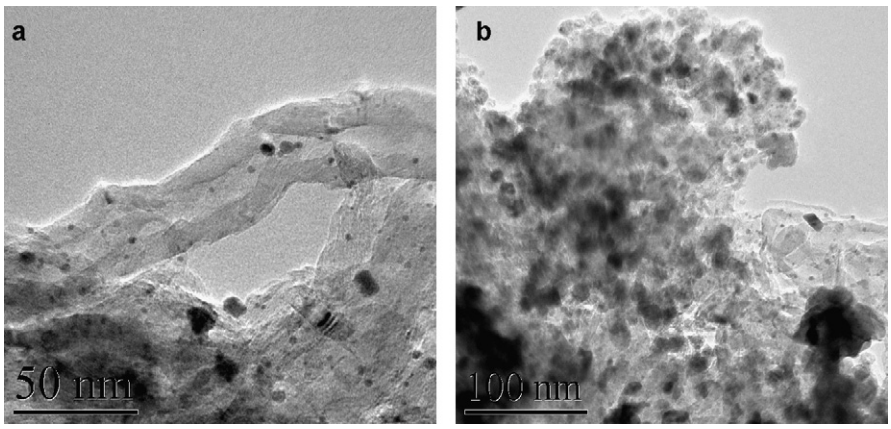

Fig. 4. TEM images of platinum catalyst supported on the most severe treated CNFs (Pt/CNF NSTb2).

was observed, although platinum particles had a similar size when compared to the particles deposited on the unoxidized CNFs [21], as seen in Fig. 3. Hence, the increase of crystallite size detected by XRD is due to the formation of agglomerates. These increase in the platinum crystallite size, or agglomeration grade, can be attributed to the decomposition of less stable surface oxygen groups during the reduction stage of the metal precursor, facilitating the mobility of platinum on the support surface and favouring the agglomeration of platinum particles [27–29]. TEM images of the Pt/CNF NSTb2 catalyst showed a broad Pt particle size distribution. Fig. 4a showed that small Pt particles were obtained where the CNFs morphology was maintained. However, the formation of large agglomerates was observed where the CNFs morphology was destroyed. On the other hand, these particles adopted a more dense globular morphology, as seen in Fig. 4b. This can be associated to a weak metal–support interaction due to the partial destruction of CNFs morphology.

Textural properties of catalysts and supports were studied by N_2-physisorption. Results are shown in Table 2. Catalysts exhibited a lower surface area and total pore volume than the corresponding carbon supports, which is attributed to the loading of the metal particles on the pore surface. In particular, a decrease of the mesoporosity was observed after the catalyst loading, indicating that platinum was mainly distributed in the mesopore structure of the support. The average pore diameter of CNFs decreased from 7 to 4 nm after the Pt deposition, confirming the distribution of metal particles on the mesopore surface. So that, the porous structure of the support is not blocked by the metal particles, favouring the diffusion of the reactant to the active sites of the catalyst.

3.3. *Electrochemical performances of Pt/CNF catalysts*

Fig. 5 shows the polarization (cell potential versus current density) and power density curves obtained for the Pt/CNF based electrode and a commercial gas diffusion electrode (E-TEK Inc.) at the anode of a PEM fuel cell. The commercial electrode was based on Pt supported on Vulcan XC-72. Pt/CNF based MEA showed a better electrocatalytic performance than the MEA based on the commercial electrode (E-TEK), because it gave lower polarization losses. Taking into account that both electrodes had the same Pt loading and Pt particle size, the better performance of the Pt/CNF based electrode may be attributed to the mesoporous structure of CNFs, which favours the triple-phase contact of reactant gas, catalyst, and the membrane, where the electrochemical reaction takes place [30,31]. Therefore, the least voltage drop with Pt/CNF based electrode may be associated to a more efficient use of metal particles. The maximum power density obtained with the Pt/CNF based electrode was 20 mW cm^{-2}. This value was about 2 times higher than that of the E-TEK based electrode (9.5 mW cm^{-2}). The power densities obtained are not too high, but it must be taken into account that the fuel cell tests were carried out at room temperature and atmospheric pressure. These power density values are similar than those obtained in the literature in the same temperature and pressure conditions.

Fig. 6 summarizes the polarization and power density curves obtained for the electrodes based on platinum supported on functionalized CNFs at the anode of a PEM fuel cell. It can be observed that all the functionalization treatments resulted in an enhancement of the cell performance. Functionalization of the support has

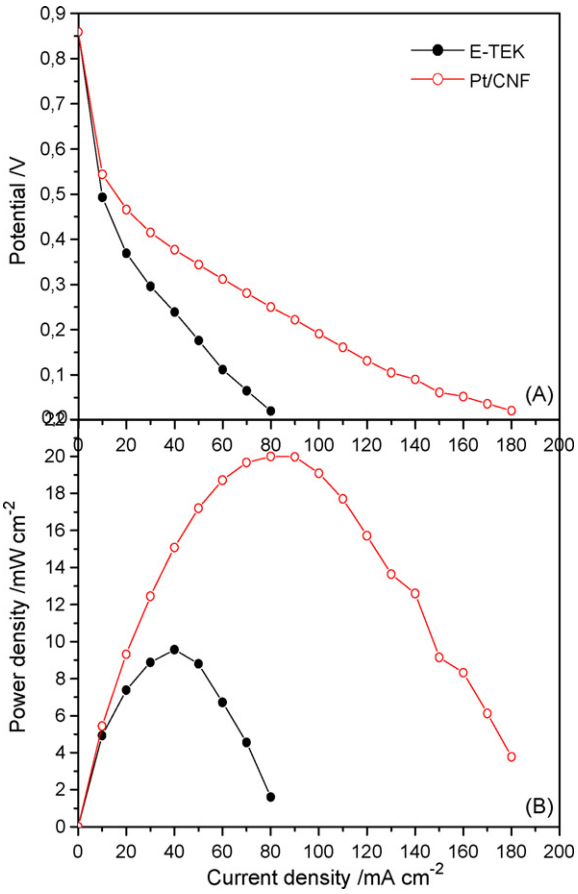

Fig. 5. Comparison of the polarization curves (a) and power densities (b) obtained using the Pt/CNF based electrode and a commercial one (E-TEK) at the anode in a PEM fuel cell at room temperature and atmospheric pressure.

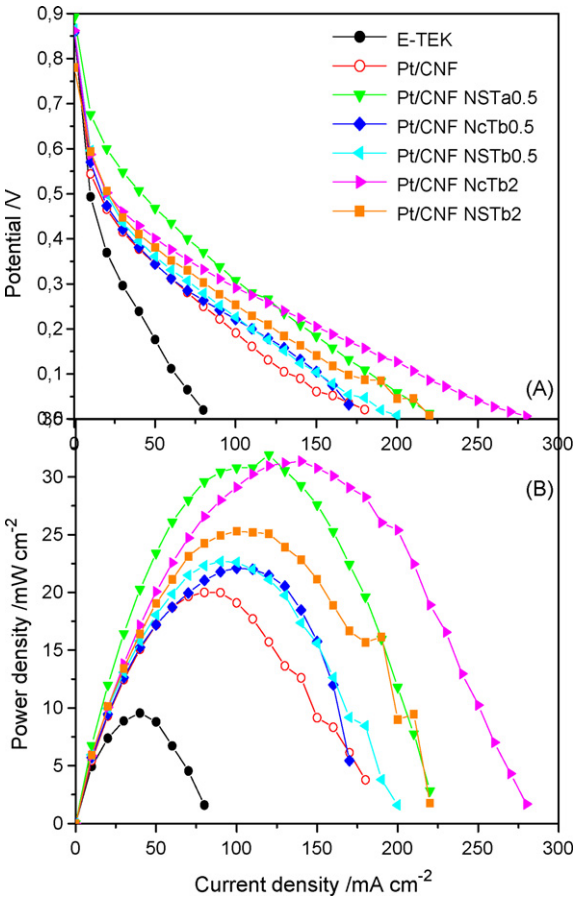

Fig. 6. Comparative performance of platinum catalysts supported on the different oxidized CNFs at the anode in a PEM fuel cell at room temperature and atmospheric pressure. (a) Polarization curves; and (b) power densities.

two opposite effects on the electrochemical performance. On one hand, it decreases the electrical conductivity of the support, which results in higher ohmic losses. But on the other hand, it improves the electron transfer from platinum to the support during the electrochemical reactions, resulting in lower ohmic losses. This transfer takes place through the oxygen atoms of the surface of the support [2]. Therefore, it is necessary to establish a compromise between the two effects in order to optimize the cell performance.

Pt/CNF NSTb0.5 catalyst gave the lowest ohmic losses. As all electrodes were tested under comparable conditions, the ohmic losses may be attributed to the different electrical conductivity of the electrode layer. In the case of electrode based on Pt/CNF NSTb0.5 catalyst, platinum was supported on CNFs that maintained the original morphology and presented a suitable surface chemistry, which improved the Pt–support interaction and did not decrease significantly the electrical conductivity of the support. However, the lowest mass transport losses were obtained with the electrode based on Pt/CNF NcTb2 catalyst. In this case, platinum is supported on CNFs with a shorter morphology. The mass transport losses may be associated with the mass transport resistance of the gas reactant through the porous structure of the electrodes. In general, catalysts supported on CNFs with a shorter morphology showed lower mass transport losses due to the better diffusion of hydrogen to the catalyst active sites through the porous structure of CNFs.

The highest power densities were obtained with Pt/CNF NSTb0.5 and Pt/CNF NcTb2 electrodes and, in both cases, were around 33 mW cm^{-2}. These catalysts were supported on carbon nanofibers with different morphology and surface chemistry. These results evidence the important effect of both the morphology and the surface chemistry of the support on the electrochemical performance of electrocatalysts. As it was explained above, these power densities are not too high. However, these values are comparable to those obtained in the literature in the same temperature and pressure conditions.

4. Conclusions

Platinum electrocatalysts supported on functionalized carbon nanofibers were prepared in order to study the influence of support properties (morphology and surface chemistry) on the preparation and performance of catalysts. The main conclusions derived from this work are as follows:

- The incipient wetness impregnation method results in an uniform distribution of the platinum particles on the mesoporous structure of CNFs. This prevents the blockage of the porous structure of the support, favouring the diffusion of the reactants.
- The size of platinum particles depends on the surface chemistry of the support. The agglomeration of platinum particles increases as the number of support oxygen groups increases. This is attributed to the decomposition of less stable surface oxygen groups during the reduction stage, which facilitates the mobility of platinum on the support surface and, thereby, favours the agglomeration of platinum particles.
- The size of platinum particles also depends on the morphology of the support. The average size of platinum particles increases as the shortening grade of CNFs increases.
- The electrocatalytic performance of catalysts depends on the morphology of the support. Catalysts supported on shortened CNFs give lower mass transport losses due to the better diffusion of hydrogen through their porous structure.
- The electrocatalytic performance of catalysts depends on the surface chemistry of the support. Functionalization of the support has two opposite effects on the activity of the catalysts. On one hand, it decreases the electrical conductivity of the support, which results in higher ohmic losses. On the other hand, it improves the electron transfer from platinum to the support during the electrochemical reactions. Therefore, it is necessary to establish a compromise between the two effects in order to optimize the cell performance.

These results are very promising. Therefore, it can be concluded that good candidates for PEMFC and DMFC can be obtained using CNFs selecting appropriate procedures for the carbon functionalization. Next steps in the current investigations will be the preparation of bimetallic catalysts to improve the performances of these materials.

Acknowledgements

The authors gratefully acknowledge financial support given by the Aragón Government under the project PM042/2007. L. Calvillo also acknowledges the Spanish National Research Council for the FPI grant.

References

[1] J.-H. Wee, K.-Y. Lee, S.H. Kim, J. Power Sources 165 (2007) 667–677.
[2] X. Yu, S. Ye, J. Power Sources 172 (2007) 133–144.
[3] X. Yu, S. Ye, J. Power Sources 172 (2007) 145–154.
[4] C.W.B. Bezerra, L. Zhang, H. Liu, K. Lee, A.L.B. Marques, E.P. Marques, H. Wang, J. Zhang, J. Power Sources 173 (2007) 891–908.
[5] Y. Shao, G. Yin, J. Zhang, Y. Gao, Electrochim. Acta 51 (2006) 5853–5857.
[6] K. Wikander, H. Ekström, A.E.C. Palmqvist, A. Lundblad, K. Holmberg, G. Lindbergh, Fuel Cells 6 (2006) 21–25.
[7] H. Tang, J. Chen, L. Nie, D. Liu, W. Deng, Y. Kuang, S. Yao, J. Colloid Interf. Sci. 269 (2004) 26–31.

[8] C. Paoletti, A. Cemmi, L. Giorgi, R. Giorgi, L. Pilloni, E. Serra, M. Pasquali, J. Power Sources 183 (2008) 84–91.
[9] J. Marie, S. Berthon-Fabry, P. Achard, M. Chatenet, A. Pradourat, E. Chainet, J. Non-Cryst. Solids 350 (2004) 88–96.
[10] N. Job, J. Marie, S. Lambert, S. Berthon-Fabry, P. Achard, Energ. Convers. Manage. 49 (2008) 2461–2470.
[11] L. Calvillo, M.J. Lázaro, E.G. Bordejé, R. Moliner, P.L. Cabot, I. Esparbé, E. Pastor, J.J. Quintana, J. Power Sources 169 (2007) 59–64.
[12] J. Ding, K.-Y. Chan, J. Ren, F.-S. Xiao, Electrochim. Acta 50 (2005) 3131–3141.
[13] Z.R. Ismagilov, M.A. Kerzhentsev, N.V. Shikina, A.S. Lisitsyn, L.B. Okhlopkova, Ch.N. Barnakov, M. Sakashita, T. Iijima, K. Tadokoro, Catal. Today 102–103 (2005) 58–66.
[14] F. Yuan, H.K. Yu, H. Ryu, Electrochim. Acta 50 (2004) 685–691.
[15] M. Tsuji, M. Kubokawa, R. Yano, N. Miyamae, T. Tsuji, M.-S. Jun, S. Hong, S. Lim, S.-H. Yoon, I. Mochida, Langmuir 23 (2007) 387–390.
[16] L. Calvillo, M.J. Lázaro, I. Suelves, Y. Echegoyen, E.G. Bordejé, R. Moliner, J. Nanosci, Nanotechnology 9 (2009), doi:10.1166/jnn.2009.MP03.
[17] T.G. Ros, A.J. van Dillen, J.W. Geus, D.C. Koningsberger, Chem-Eur. J. 8 (2002) 1151–1162.
[18] M.L. Toebes, J.M.P. van Heeswijk, J.H. Bitter, A.J. van Dillen, K.P. de Jong, Carbon 42 (2004) 307–315.
[19] A. Guha, W. Lu, A. Zawodzinski Jr., D.A. Schiraldi, Carbon 45 (2007) 1506–1517.
[20] J. Guo, G. Sun, Q. Wang, G. Wang, Z. Zhou, S. Tang, L. Jiang, B. Zhou, Q. Xin, Carbon 44 (2006) 152–157.
[21] F. Zaragoza-Martín, D. Sopeña-Escario, E. Murallón, C. Salinas-Martínez de Lecea, J. Power Sources 171 (2007) 302–309.
[22] I. Suelves, M.J. Lázaro, R. Moliner, B.M. Corbella, J.M. Palacios, Int. J. Hydrogen Energ. 30 (2005) 1555–1567.
[23] J.L. Figueiredo, M.F.R. Pereira, M.M.A. Freitas, J.J.M. Orfao, Carbon 37 (1999) 1379–1389.
[24] C. Suryanarayana, M.G. Norton, X-ray Diffraction: A Practical Approach, Plenum Press, New York and London, 1998, pp. 207–221.
[25] P. Serp, M. Corrias, P. Kalck, Appl. Catal. A: Gen. 253 (2003) 337–358.
[26] C.A. Bessel, K. Laubernds, N.M. Rodríguez, R.T.K. Baker, J. Phys. Chem. B 105 (2001) 1115–1118.
[27] A. Sepúlveda-Escribano, F. Coloma, F. Rodríguez-Reinoso, Appl. Catal. A: Gen. 173 (1998) 247–257.
[28] M.C. Román-Martínez, D. Cazorla-Amorós, A. Linares-Solano, Carbon 33 (1995) 3–13.
[29] F. Coloma, A. Sepúlveda-Escribano, J.L.G. Fierro, F. Rodríguez-Reinoso, Langmuir 10 (1994) 750–755.
[30] R. O'Hayre, D.M. Barnett, F.B. Prinz, J. Electrochem. Soc. 152 (2005) A439–A444.
[31] G.G. Scherer, Solid State Ionics 94 (1997) 249–257.